



ASIA **TURBOMACHINERY** & **PUMP** SYMPOSIUM
12 - 15 MARCH 2018
SUNTEC SINGAPORE

SUBSYNCHRONOUS VIBRATIONS ON A VERTICAL ELECTRICAL MOTOR DURING FACTORY TESTING – OBSERVED PHENOMENON, INTERPRETATION AND RESOLUTION

Dr Alain GELIN

Senior Rotating Equipment
TOTAL E&P
64000 Pau, France

Bernard QUOIX

Senior Fellow - Head of Rotating Machinery Department
TOTAL E&P
64000 Pau, France

C. Hunter CLOUD

President
BRG Machinery Consulting
Charlottesville, Virginia US

Dr Minhui HE

Machinery Specialist
BRG Machinery Consulting
Charlottesville, Virginia



Dr. Alain GELIN is Senior Rotating Equipment engineer at TOTAL E&P Head Quarter in Pau, France. He is involved in the development schemes for compression, pumping and power generation systems and he supports projects and site trouble shooting activities as well. He is also deeply involved in qualification programs for new equipment and his expertise covers all mechanical aspects such as rotordynamics, aerodynamics, lubrication, magnetic bearings, stress and modal analysis, LNG compressors, testing, condition monitoring. He joined TOTAL in 2005, and previously had worked 20 years for GE Oil & Gas (former Thermodyne) where he was successively R&D Mechanical Engineer and Testing Department Manager for both Steam Turbine and Centrifugal Compressor applications. He has authored 15+ technical papers in dynamics and he is member of the IFToMM committee. Dr. GELIN obtained his Master's Degree (1986) and his Ph.D. (1989) at INSA Lyon.



Bernard QUOIX is the Head of TOTAL E&P Rotating Machinery Department and holds this position since November 2003. He started his career in 1979 within TOTAL Operations in the North Sea, then from 1986 to 1989 became Head of Engineering of Turbomeca Industrial Division, a small and medium size gas-turbines manufacturer, then went to Renault Car Manufacturer as Assistant Manager of the engine testing facilities, before joining Elf Aquitaine and eventually TOTAL, mainly involved in all aspects of turbomachines, including conceptual studies, projects for new oil and gas field development, commissioning and start-up, and bringing his expertise to operations of all TOTAL affiliated companies worldwide. Bernard QUOIX graduated from ENSEM (Ecole Nationale Supérieure d'Electricité et de Mécanique) in Nancy (France) in 1978 and then completed his engineering education with one additional year at ENSPM (Ecole Nationale du Pétrole et des Moteurs) in Paris, specializing in Internal Combustion Engines. Bernard QUOIX is a member of the Turbomachinery Advisory Committee since 2005, and is also the President of ETN (European Turbine Network), organization based in Brussels, since 2010 and Vice president of Association Française de Mécanique (AFM), based in Paris, since 2013. In October 2015, Bernard QUOIX was nominated Senior Fellow of TOTAL in the area of Rotating Machinery by TOTAL's CEO.



C. Hunter CLOUD is President of BRG Machinery Consulting, LLC, in Charlottesville, Virginia, a company providing a diverse range of rotating machinery technical services. He began his career with Mobil Research and Development Corporation in Princeton, NJ, as a turbomachinery specialist responsible for application engineering, commissioning, and troubleshooting for production, refining and chemical facilities. During his 11 years at Mobil, he worked on numerous projects, including several offshore gas injection platforms in Nigeria as well as serving as reliability manager at a large US refinery.

Dr. Cloud received his B.S. (Mechanical Engineering, 1991) and Ph.D. (Mechanical and Aerospace Engineering, 2007) from the University of Virginia. He is a member of ASME, the Vibration Institute, the API 617 and API 684 task forces, and the advisory committee for the Texas A&M Turbomachinery Symposium.



ASIA TURBOMACHINERY & PUMP SYMPOSIUM
12 - 15 MARCH 2018
SUNTEC SINGAPORE



Minhui HE is a Machinery Specialist with BRG Machinery Consulting LLC, in Charlottesville, Virginia. His responsibilities include vibration troubleshooting, rotordynamics analysis, as well as bearing and seal analysis and design. He is also conducting research on rotordynamics and hydrodynamic bearings.

Dr. HE received his B.S. degree (Chemical Machinery Engineering, 1994) from Sichuan University, China. From 1996 to 2003, he conducted research on fluid film journal bearings in the ROMAC Laboratories at the University of Virginia, receiving his Ph.D. (Mechanical and Aerospace Engineering, 2003). He is a member of ASME and the advisory committee for the Texas A&M Asia Turbomachinery and Pump Symposium.

ABSTRACT

During the factory tests of a vertical electric driven de-ballasting pump, casing vibrations were observed on the motor above the contractual limit of 2.8 mm/s, mainly on the motor's top, Non-Drive End. Supported by fluid film journal bearings, this motor is cooled and lubricated by a low viscosity fluid in which the entire rotor assembly is submerged. A spectrum analysis revealed that the dominant vibration was a subsynchronous component near 12.5 Hz, corresponding to half of the rotating frequency. However, the motor was not equipped with proximity probes and therefore no information on the shaft vibrations was available.

Initial investigations included geometrical and dimensional checks which did not reveal any evidence of defects. A modal analysis of the motor casing, both theoretical and experimental, confirmed the location of the casing's reed frequency mode at approximately 12.5 Hz.

Given these modal testing results, the motor was retested with additional bracing located on the Non-Drive End side (top of the motor). The vibrations amplitude decreased, but was still present. The motor was then equipped with proximity probes to measure the relative displacement at both shaft ends. Results clearly showed very high vibrations displacement of 200 μ m p-p at exactly half of the rotating frequency, whatever the speed, and these levels represented around 90% of the bearings clearance! With these test results, it became clear that the root cause of the casing subsynchronous vibrations was a rotor whirl instability exciting the motor's reed frequency mode. This paper will describe a detailed rotordynamics analysis from which the results indicated the presence of two rotor modes very close in frequency and tracking the half running speed, predicted to be unstable whatever the speed, confirming the observed fluid whirl phenomenon with amplitudes largely exceeding API vibration criteria. For historical reference and interest, thirty years ago, Ed Gunter was involved in fixing vertical pumps for the US Navy that used plain journal bearings and consequently whirled [1].

Modifications to the bearings design appeared then to be mandatory, which will be described in the paper, including a detailed rotordynamics comparative analysis between the two configurations. Finally, both the analysis results and the tests results with these modified bearings proved to be fully consistent and eventually solved the initial observed subsynchronous shaft instability.

INTRODUCTION

Induction electrical motors are widely used in the Oil & Gas industry to drive process compressors including centrifugal, reciprocating and screw types or to drive water injection pumps or oil export pumps. In addition, electrical motors are also used for sea water lift pumps, air compressors, hydraulic power units, cooling water loop, preservation units and to drive different types of auxiliary pumps for services such as chemical products, methanol injection etc.

This lecture deals with a very particular type of electrical motors used to drive de-ballasting pumps for floating offshore supports like semi sub platforms. The main function of these motor-pumps is to maintain the draught during normal operation and to restore the platform to its upright position during transient conditions. The technology of these vertical de-ballasting motor-pumps is derived from the well proven OH4 design as per API 610 [11], knowing that this technology is not suitable for submerged conditions.



ASIA **TURBOMACHINERY** & **PUMP** SYMPOSIUM
12 - 15 MARCH 2018
SUNTEC SINGAPORE



Figure 1: Standard OH4 motor-pump (left) as per API 610 versus de-ballasting submerged motor pump (right)

The de-ballasting motor pumps are designed to be able to work in a fully submerged environment; it is the reason why the design of the electrical motor is completely different from OH4 standard design. The IP68 wet wound motor is not cooled at atmospheric pressure, but it is fully flooded with a low viscosity lubricant for bearing lubrication and cooling purpose. The cooling media is usually a mixture of water and glycol or low viscosity oil. In addition, a small centrifugal circulation impeller is installed onto the motor or pump shaft to circulate the cooling/lubricating media and thus to refresh the whole equipment. As the complete assembly is installed in the vertical position, a thrust bearing is also used and lubricated with the same low viscosity lubricant. A dedicated seal is installed at the motor Non-Drive End (NDE) and bottom side to avoid the migration of cooling/lubricant media into the environment. On the pump side, another seal cartridge is used to avoid the migration of sea water (pumping product) to the environment. With such a technology, the motor-pump is able to normally work in a dry machinery room but it is also able to work in a fully submerged environment when the tilting of the platform is such that its horizontal position needs to be recovered. This equipment is installed into machinery rooms at the bottom four corners of the floating installation to manage the sea water de-ballasting if required due to external temporary loads.

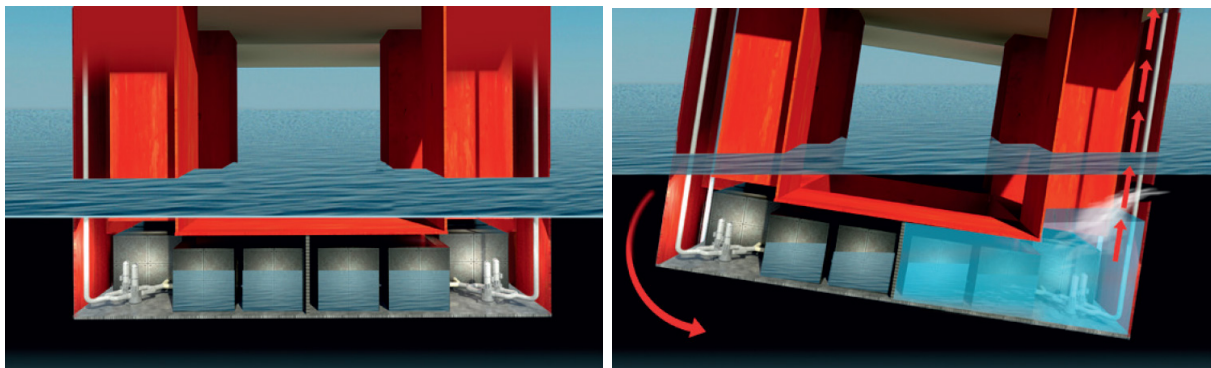


Figure 2: Principle of operation of de-ballasting motor-pump system



ASIA **TURBOMACHINERY** & **PUMP** SYMPOSIUM
12 - 15 MARCH 2018
SUNTEC SINGAPORE

TOTAL is involved in a project requiring 12 de-ballasting motor-pump assemblies, 3 packages being installed into each 4 piles of a semi submersible platform. The main characteristics of each package are as follows:

Motor rated power: 400 kW

Rotating speed: 1500 rpm

Duty: sea water, 630 m³/h capacity, 110 m differential head

Vertical arrangement

Motor cooling/lubricant media: water (65%) / Glycol (3%) with a kinematic viscosity around 2 cSt at 40°C

Cylindrical bearing with 3 axial feeding groove

Tilting pad thrust bearing on active downward side, and fixed geometry on inactive upward side

No permanent monitoring system for vibration

Each Non-Drive End (NDE) side on top and Drive End (DE) side bottom journal bearings are equipped with 2 cylindrical sleeves, remembering also that the shaft line and the motor rotor are installed in the vertical direction without any radial load (see Figure 3 represented in the horizontal direction). Figure 3 shows some details, and the following sub-equipment are identified from left to right: the extended shaft for pump assembly (not represented), the intermediate bottom bearing, the seal cartridge, the thrust bearing, the circulating impeller, the DE (bottom) double journal bearing sleeves, the motor and the NDE (top) double journal bearing sleeves.

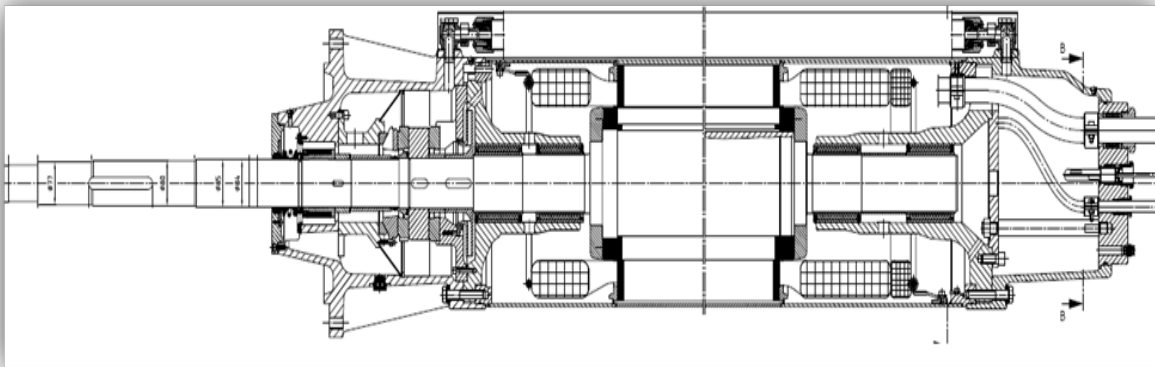


Figure 3: Cross section drawing of the motor



ASIA **TURBOMACHINERY** & **PUMP** SYMPOSIUM
12 - 15 MARCH 2018
SUNTEC SINGAPORE

PROBLEM STATEMENT

De-ballasting vertical motor-pumps are very critical equipment for the stability of the asset and it is the reason why all 12 complete assemblies were tested in full load conditions. All packages were installed in the dry testing room and the overall performances were measured using a dedicated water closed loop to load the motors (see Figure 4).

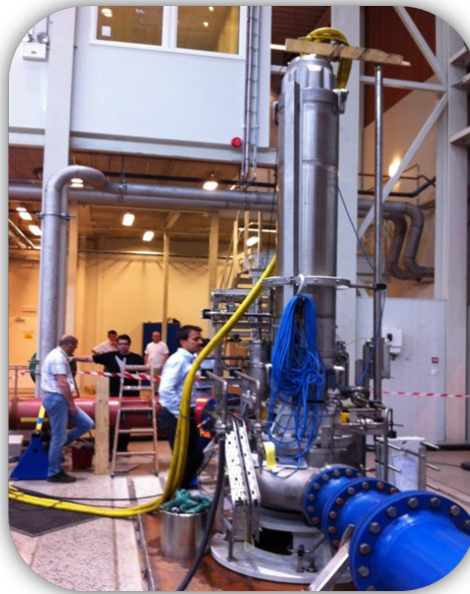


Figure 4: Complete assembly during load test

During the load test, all motors were equipped with five (5) accelerometers to record vibration levels:

- 2 radial X and Y accelerometers on NDE side (top)
- 2 radial X and Y accelerometers on DE side (bottom)
- 1 axial accelerometer on NDE side

As this type of motor is so particular (vertical arrangement, low viscosity cooling and lubricant fluid, submerged assembly, etc.), there is no existing standard to cover the acceptance vibration criteria during mechanical running tests and performance tests. The closest reference for such equipment is probably the ISO 10816-Part 7, and from table A-1 (Zone A, Category 1, > 200 kW) [12] for newly commissioned machines in the preferred operating range, the acceptance level is 3.5 mm/s rms at bearing housing locations.

Table 1 summarizes the casing vibration levels recorded during load tests. The vibrations exceed the criteria on 6 units among 12. The frequency analysis show that the overall levels are mostly due to the participation of a subsynchronous component very close to half of the rotation frequency ($0.5\times$) at around 12.5 Hz. For some spectra, as per those recorded on Unit 11, only the $0.49\times$ component is observed as shown in Figure 5.

Due to the high content of subsynchronous casing vibrations, the behavior of the units was considered unacceptable putting at stake the integrity of the whole assembly, and further investigations were required.



ASIA **TURBOMACHINERY** & **PUMP** SYMPOSIUM
12 - 15 MARCH 2018
SUNTEC SINGAPORE

	NDE - Upper			DE - Lower		
	Synchronous	Sub-Synchronous	Overall	Synchronous	Sub-Synchronous	Overall
	1 X	~0,48 X	10 - 1kHz	1 X	~0,48 X	10 - 1kHz
	mm/s rms	mm/s rms	mm/s rpm	mm/s rms	mm/s rms	mm/s rpm
Unit 1	0,70	0,89	1,13	0,10	1,26	1,26
Unit 2	0,40	0,40	0,57	0,10	0,38	0,39
Unit 3	0,35	3,64	3,66	0,10	1,89	1,89
Unit 4	0,32	0,71	0,78	0,49	1,01	1,12
Unit 5	0,10	3,22	3,22	0,49	4,57	4,60
Unit 6	0,67	1,00	1,20	0,64	2,65	2,73
Unit 7	0,10	3,64	3,64	0,35	5,11	5,12
Unit 8	0,42	0,10	0,43	0,10	0,10	0,14
Unit 9	0,53	3,52	3,56	0,10	2,13	2,13
Unit 10	0,46	0,85	0,97	0,10	0,82	0,83
Unit 11	0,10	4,14	4,14	0,10	5,21	5,21
Unit 12	0,10	4,62	4,62	0,10	1,12	1,12

Table 1: Casing vibrations during load test – acceptance level criteria 3.5 mm/s rms

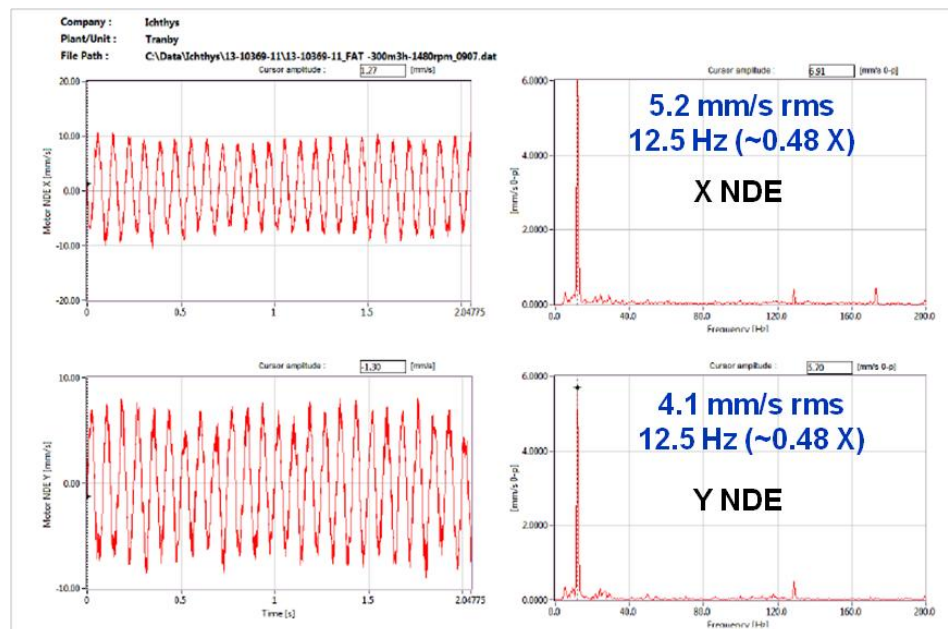


Figure 5: Casing vibration on Unit 11 – time frame and spectra



ASIA **TURBOMACHINERY** & **PUMP** SYMPOSIUM
12 - 15 MARCH 2018
SUNTEC SINGAPORE

INVESTIGATION

First of all, an experimental analysis was conducted to identify the natural frequencies of the assembly. A shock hammer equipped with a force transducer was used to excite the complete assembly. The dynamic response to the excitation was measured and the transfer function between the upper accelerometer signals related to the injected force was extracted (see Figure 6). The first natural frequency corresponding to the first bending mode of the complete assembly installed in the test bed was clearly identified around 12.5 Hz. The mode shape and the natural frequency were also confirmed by a Finite Element modal analysis using realistic boundary condition at motor bottom flange fixation point (see also Figure 6).

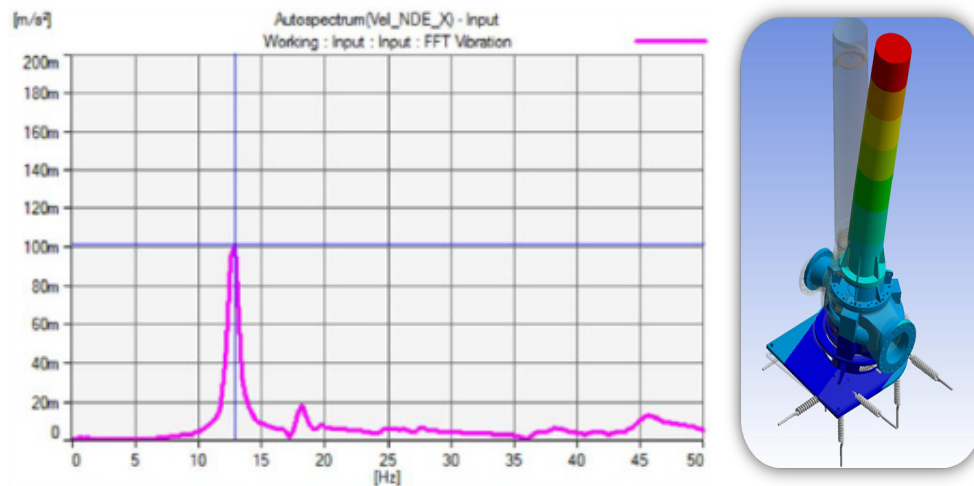


Figure 6: Experimental and theoretical modal analysis – natural frequency around 12.5 Hz (~0.48×)

To confirm the influence of the casing natural frequency on the vibration levels, a temporary upper bracing was installed on the NDE side. The objective of this clamping system was to implement an additional stiffness into the dynamic system at the main deflecting point. The upper bracing was based on four (4) U-shape solid beams to block the NDE side as shown in Figure 7. The bump test was repeated with the upper bracing and, thanks to the additional stiffness, the natural frequency moved from about 12.5 Hz to roughly 20 Hz. The load test was thus repeated on Unit 11, the one that had previously shown the higher vibrations, and with the upper NDE clamping system, the vibration levels decreased from more than 5 mm/s rms to less than 1 mm/s rms, but still with a very low indication of the subsynchronous activity.



ASIA **TURBOMACHINERY** & **PUMP** SYMPOSIUM
12 - 15 MARCH 2018
SUNTEC SINGAPORE



Figure 7: Complete assembly with upper clamping system during load test

From the previous investigations (modal analysis and casing vibration measurements with and without upper bracing), it clearly appeared that the first bending mode of the complete assembly which is located at 12.5 Hz was excited by an excitation mechanism at about half rotating speed. Shifting the casing natural frequency had a clear impact on the response of the system from a casing vibration standpoint, but did not explain the origin of the excitation mechanism at $0.48\times$. Unfortunately the motor was not equipped with any proximity probes and the rotor behavior inside the motor casing was unknown.

As the motor is entirely flooded with cooling/lubricant water/glycol media, some assumptions were issued to tentatively explain the root cause of the observed casing vibration. Among these assumptions, the motor bearing arrangement was firstly investigated, also because the shaft line vertical direction installation without any (or with very low) radial load.

On both NDE and DE sides, the motor is equipped with 2 concentric and cylindrical bearing sleeves with insert bushing made of hard carbon to allow some contacts during transient phases such as startup and coast down. Three axial grooves are machined at Inner Diameter (ID) of the cylindrical bushes for feeding purpose of the water and glycol lubricant mixture. The nominal diameter of the bearing is 110 mm while its length is 100 mm. The minimum and maximum clearances are respectively 0.220 / 0.304 mm (in diameter) corresponding to 2.00 o/oo and 2.76 o/oo non-dimensional clearances.

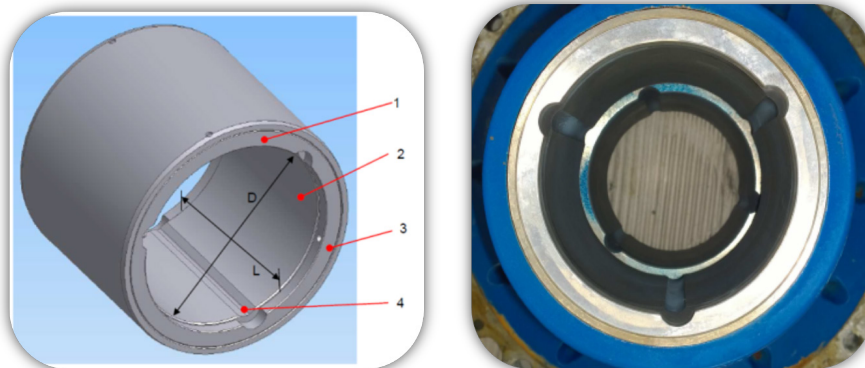


Figure 8: Bearing configuration

Copyright© 2018 by Turbomachinery Laboratory, Texas A&M Engineering Experiment Station



To better understand the motor rotor behavior inside the bearings and to measure the rotor to casing relative shaft displacements, 2 sets of Bently Nevada proximity probes were installed on NDE and DE sides in between the two bearing sleeves in X and Y directions. The measurements were performed without and with the upper bracing. Figures 9 shows the spectra recorded on the NDE upper side with and without upper bracing. The same behavior was recorded on DE bottom side: Both X and Y vibrations at NDE and DE sides are purely subsynchronous at exactly $0.5\times$ with or without bracing. The orbits are purely circular running at half of the rotating frequency in the forward direction, and the amplitudes of the vibrations were around $200\text{ }\mu\text{m}$ peak to peak, which represent more or less 75% of the mean bearing clearance.

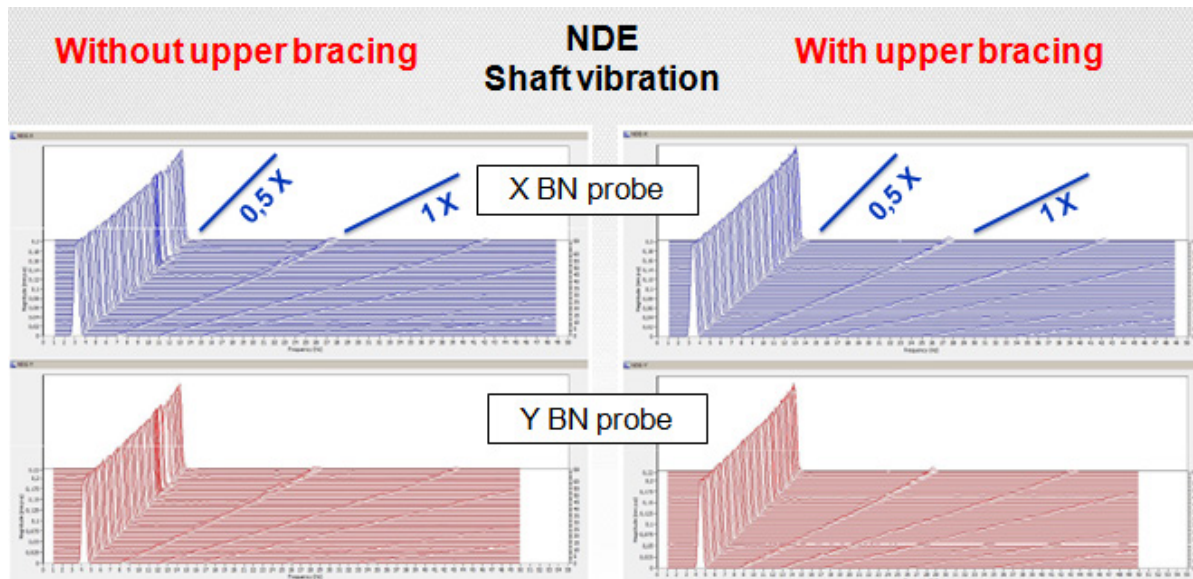


Figure 9: Shaft to casing vibrations $\sim 200\text{ }\mu\text{m}$ peak to peak at $0.5\times$, with and without upper bracing

Even if the motors are not normally equipped with proximity probes, such high vibrations level are clearly not acceptable. General standards such as API or IEC specify around $20\text{--}25\text{ }\mu\text{m}$ peak to peak for non synchronous vibrations. In addition, and even if the bearing sleeves are made of hard carbon epoxy impregnated, some wearing mechanisms can be induced with such amount of vibrations, and the most critical components for long term operation are without any doubts the sealing cartridges.

From a pure bearing stability standpoint and as indicated in many literatures, cylindrical bearings are well known to be the less stable configuration especially for low radial load (vertical configuration), large clearance and low viscosity lubricant. In such circumstances, such bearings can promote oil whirl mechanism at a little less than $0.5\times$. See for example API 684 [13] (tutorial on rotordynamics) paragraph 2.5.3: “Fixed geometry or sleeve bearings have the annoying properties of creating an excitation force that can drive the rotor unstable by creating sub-synchronous vibration. This phenomenon usually occurs at relative high speeds and/or light bearing loads, or, more generally at High Sommerfeld numbers. The problem is that sleeve bearings (i.e., all journal bearings excluding tilting pad bearings) support a resultant load with a displacement that is not directly in line from the load force. This angle can approach 90° for light load and high speed which results in high cross-coupling forces that may drive the rotor unstable”.

Getting the confirmation of the bearing whirling mechanism and the rotor unstable behavior, the motor-pumps were rejected. Proper modifications were requested to cure the subsynchronous vibration issue that was putting at stake the stability of the semi sub platform and the Project.



ASIA **TURBOMACHINERY** & **PUMP** SYMPOSIUM
12 - 15 MARCH 2018
SUNTEC SINGAPORE

ROTORDYNAMICS ANALYSIS

In order to understand the vibration phenomena being encountered, as well as determining what modifications will help to resolve the problem, dynamic models of the following components and effects were developed for the motor:

- Rotor assembly
- Casing assembly
- Three axial groove bearings (2 on either side of motor core)
- Plain sleeve, bottom support bearing
- Fluid “air” gap between rotor and stator

The rotor and casing assemblies were modeled using beam finite elements. Figure 10 presents these two models along with the five journal bearing locations that provided the interconnections. At the casing’s bottom mounting flange, radial and moment stiffness were used to connect the casing to the ground. Since the motor’s reed frequency was well established from the above mentioned measurements, a complex finite element analysis of the mounting flange was not necessary to determine its stiffness. Instead, the moment stiffness to the ground was adjusted to match the measured reed frequency at 720 cpm (12 Hz).

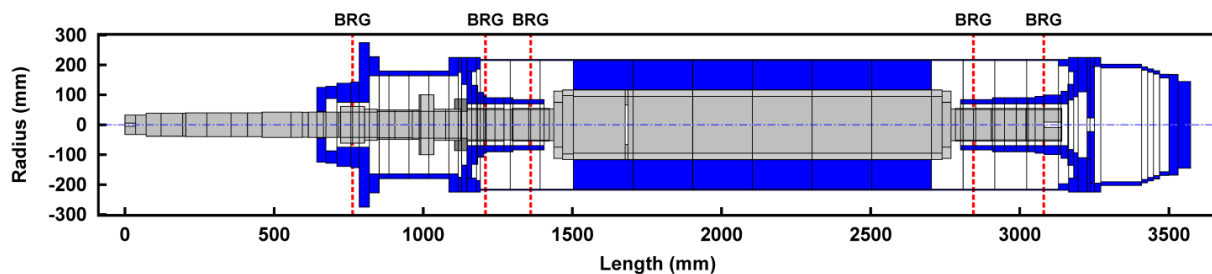


Figure 10: Schematic of rotor assembly and casing assembly models

Lubricated by the same water-glycol mixture that cools its electrical core, the motor’s fixed geometry bearings were modeled using a proprietary finite element code based on theories and methods developed in [2]. The bearings’ submerged condition requires that the lubricant’s surrounding ambient pressure be considered in the analysis, which allows for suppression of cavitation within the bearing film.

As illustrated in Figure 11, when cavitation is totally suppressed in a plain cylindrical bearing, the fluid film provides no radial force as the shaft is radially perturbed. Only a tangential force on the shaft is created due to the resulting symmetric positive and negative pressure fields. In other words, suppressing cavitation causes a plain cylindrical bearing to produce only pure cross-coupled stiffness and no direct stiffness, both of which promote self-excited instabilities.

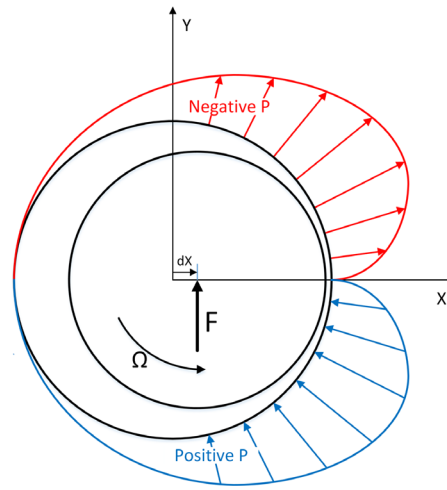


Figure 11: Film pressures within an uncavitated, plain cylindrical bearing

Table 2 presents the calculated dynamic coefficients of the motor's bearings at operating speed and average clearance condition. The bearings' vertical, lightly loaded and submerged condition results in relatively low direct stiffness values. As expected, the bearings' fluid films provide little radial support and generate mostly destabilizing cross-coupling. Virtual added mass terms, also shown in Table 2, were determined as part of the analysis to help account for fluid inertia effects due to the low viscosity water-glycol mixture acting as the lubricant [3].

Dynamic Component	3 Axial Groove Bearing	Plain Sleeve Bottom Bearing	Fluid Air Gap
K_{xx} (N/mm)	-887	0	-23062
K_{xy} (N/mm)	2864	5425	23796
K_{yx} (N/mm)	-3131	-6066	-23796
K_{yy} (N/mm)	771	0	-23062
C_{xx} (N-s/mm)	41	78	307
C_{xy} (N-s/mm)	5	0	595
C_{yx} (N-s/mm)	5	0	-595
C_{yy} (N-s/mm)	37	69	307
$M_{xx} = M_{yy}$ (kg)	0.124	0.092	3840

Table 2: Calculated dynamic properties of bearings and fluid air gap at 1480 rpm

Dynamic effects of the motor's fluid-cooled "air" gap were determined based on the works of Fritz [4] and Black [5]. Table 2 illustrates the very significant dynamics created by this fluid air gap. Large virtual mass and negative direct stiffness terms are produced due to fluid inertia and Bernoulli effects. Furthermore, large cross-coupled stiffness is created due to the gap acting like a long, non-cavitating plain sleeve bearing with behavior like that shown in Figure 11.

With all the dynamic components and effects assembled into a single system, a damped eigenvalue or stability analysis was performed as a function of the motor's speed. Figure 12 presents the results of this type of analysis that was originally introduced to the rotordynamics community by Lund [6]. Unlike the $1\times$ line that is associated with an excitation source (e.g., unbalance), the $0.5\times$ line is strictly shown for reference, as it is not associated with an independent excitation source.

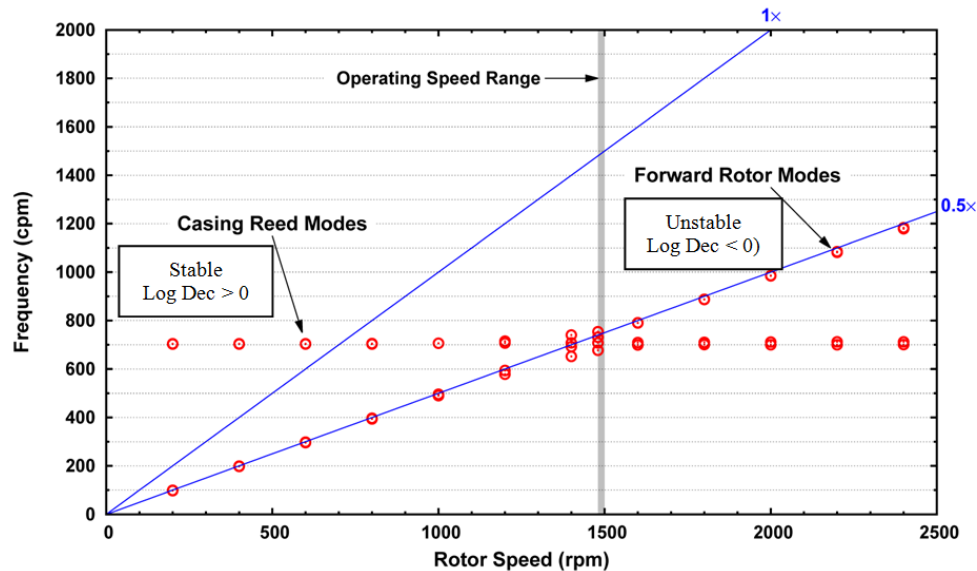


Figure 12: Damped Campbell diagram of motor system's lateral dynamics

Two sets of modes are present within Figure 12's speed/frequency range: two casing reed modes and two forward rotor modes. The modes associated with the casing's reed frequencies (two, almost identical in frequency) remain constant with speed. Figure 13 illustrates why these modes earn their so-called "reed" name due to the entire motor casing vibrating like a reed of grass supported only at the ground. Such behavior was also predicted using the more complex finite element model of the entire motor-pump casing shown in Figure 6. With one mode whirling in the forward direction and the other in the backward direction, both reed frequency modes are very lightly damped, as one would expect for structural modes.

Unlike the reed modes, the two rotor modes are shown to be highly speed dependent in Figure 12's Campbell diagram. Both modes closely track the motor's speed at frequencies just below the 0.5 \times reference line. Figure 14 also indicates that both rotor modes are highly unstable with large negative log decrement levels. Even at 200 rpm, both rotor modes possessed negative log decrement values throughout the speed range of Figure 12. Similar results were obtained for the range of bearing clearances and expected cooling fluid temperatures. These rotor modes' unstable damping levels, forward whirling direction, and 0.5 \times tracking behavior correlate well with Figure 9's subsynchronous vibration measurements and indicate that the motor is experiencing "oil whirl" instability.

Ninety years after Newkirk and Taylor published the first account of oil whirl [8], it remains one of the most misunderstood vibration phenomenon. Many recognize the behavior and associate it correctly with a self-excited instability. However, a common thinking is that it is an instability caused by a breakdown of the oil film that creates a *forced* excitation on the shaft with 0.5 \times frequency, an excitation frequency that is believed to be totally unrelated to the rotor's natural frequency and independent of rotor vibration. When this fluid film excitation frequency coincides with the rotor's natural frequency, the thinking is that a shaft whip instability is created and remains "locked" on the rotor's natural frequency. The term "locked" brings the connotation that some other excitation frequency exists within the oil film that is independent of the rotor's natural frequency.

In reality, both oil whirl and shaft whip are self-excited instabilities of the same rotor natural frequency, i.e., the rotor's first forward whirling mode. Contrary to the common thinking described above, neither phenomenon is caused by the presence of some forced excitation with its own frequency independent of the rotor's natural frequencies. Both phenomena occur because system dynamics cause the rotor's first forward mode to have inadequate damping or a negative log decrement.



ASIA **TURBOMACHINERY** & **PUMP** SYMPOSIUM
12 - 15 MARCH 2018
SUNTEC SINGAPORE

The basic recipe to produce oil whirl is to operate a fixed geometry bearing in an unloaded condition where the journal is centered with little to no eccentricity. In this situation, the oil film does not, as many seem to believe, “breakdown” or “collapse” creating some fluid disturbance within the film that has a forcing frequency of $0.5\times$. Instead, the oil film at low shaft eccentricities simply generates almost no positive direct stiffness along with relatively high cross-coupled stiffness. This is illustrated by the bearing coefficients in Table 2.

Furthermore, all fixed geometry bearing designs do not generate oil whirl instabilities when operated at light static loads. Plain cylindrical bore sleeve bearings are the most susceptible, but other fixed geometry designs can be immune to oil whirl (not necessarily shaft whip) because of their ability to produce large direct stiffness. Likewise, tilting pad journal bearings do not succumb to oil whirl at low eccentricities, making them a popular choice for vertical applications.

Oil whirl is a well-recognized concern for vertical applications incorporating fixed geometry-like bearings. This was first realized by Newkirk and Kimball [7] in their vertical test rig. More recently, the problem was reported on a vertical motor [8] and a vertical motor-pump configuration similar to the subject machine [9]. However, for the subject machine, the original high casing vibrations were being caused by a rather unusual “perfect storm” in a vibration sense, *i.e.*, a self-excited instability causing a resonance situation at running speed. Basically, oil whirl was exciting the motor’s reed frequency when the motor reached operating speed. Measurements and rotordynamics analysis confirmed this behavior, providing strong confidence that the root cause of the vibration problems, *i.e.*, oil whirl, could not be eliminated by simply shifting the motor casing’s reed frequency with additional supports.

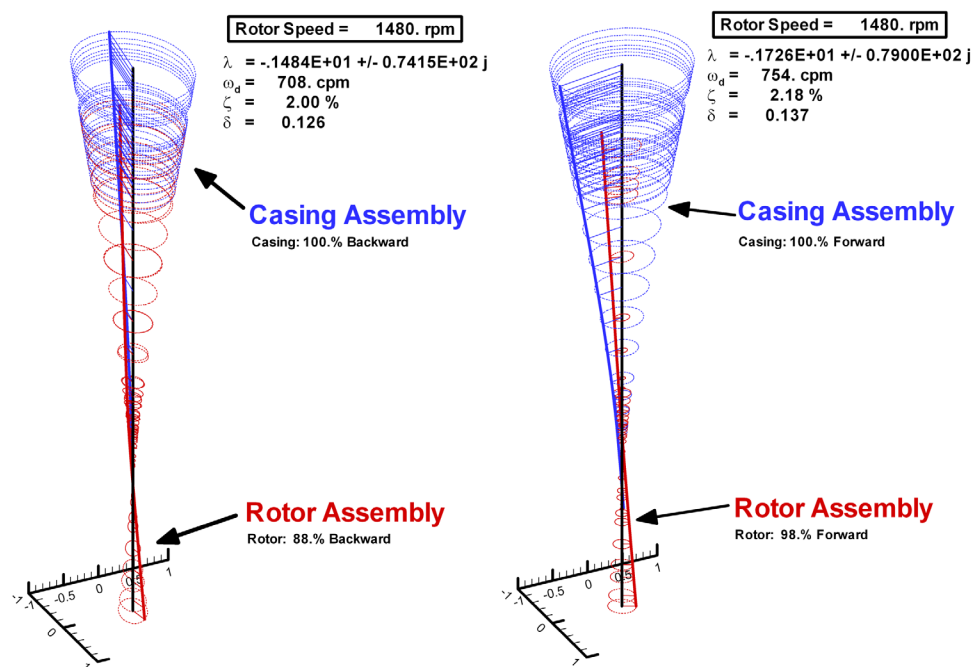


Figure 13: Reed modes of motor assembly

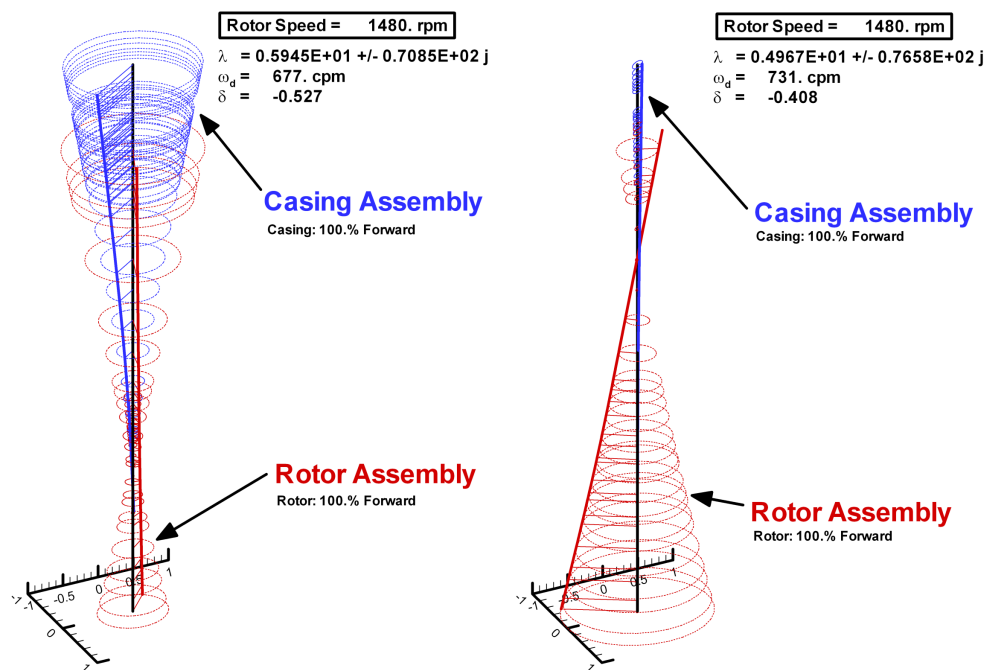


Figure 14: Rotor modes of motor assembly



ASIA **TURBOMACHINERY** & **PUMP** SYMPOSIUM
12 - 15 MARCH 2018
SUNTEC SINGAPORE

BEARING MODIFICATIONS

As confirmed by the rotordynamics calculation, the original bearing configuration promotes the oil whirl at half frequency. The shaft line arrangement with the vertical configuration and the low viscosity lubricant (roughly 20 times lower than standard mineral oil such as ISO VG 32/46) are two aggravating factors.

As the pure cylindrical configuration is known as the worst configuration from a bearing stability standpoint, promoting oil whirl, a new bearing design was investigated. Due to space constraint it was not possible to implement the “best in class” tilting pad bearing configuration to avoid any cross coupling stiffness. It is the reason why, and as also recommended by API 684 [13], a taper land bearing was designed with three taper and offset pockets. The bearing trailing part over 20° remained cylindrical with a smooth transition (purely tangential) between the lobes and the cylindrical part. To increase furthermore the impedance of the bearing (with higher direct stiffness and damping coefficients), the clearance was also reduced and side lands were implemented to combine the effect of a pressure dam bearing over the three lobes. The typical geometric is shown in Figure 15.

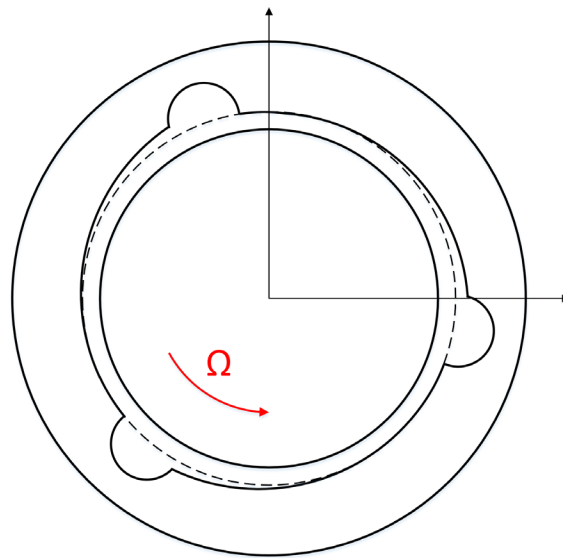


Figure 15: Schematic of an offset, three lobe bearing

The new bearing configuration being as follows:

- Similar axial supply groove (over 10° as per original design)
- Three lobe offset with a geometrical preload coefficient of 0.5 over 90°
- Trailing cylindrical part over 20°
- Reduced clearance of 0.140 to 0.220 mm (in diameter) or 1.40 to 2.00 o/oo (versus original 2.00 to 2.76 o/oo)
- Two side lands of few millimeters thickness
- Material as per original one (hard carbon epoxy impregnated)



Figure 16: New bearing sleeve (three lobes with offset)

Table 3 compares the dynamic characteristics of the original plain cylindrical, three axial groove bearing and those of the modified design incorporating offset. The most notable difference is the large increase in direct stiffness that is provided by the modified design. This is a direct result of the modified design's significantly higher oil film pressures, illustrated in Figure 17. Unlike the original plain cylindrical design, the offset lobes' converging wedges generate significant film pressures, regardless of the journal position. A converging wedge is one of the key ingredients for generating hydrodynamic pressure [10].

Dynamic Component	Original	Modified
K_{xx} (N/mm)	-887	5202
K_{xy} (N/mm)	2864	3010
K_{yx} (N/mm)	-3131	-2745
K_{yy} (N/mm)	771	6696
C_{xx} (N-s/mm)	41	43
C_{xy} (N-s/mm)	5	5
C_{yx} (N-s/mm)	5	5
C_{yy} (N-s/mm)	37	49
$M_{xx} = M_{yy}$ (kg)	0.124	0.16

Table 3: Calculated dynamic properties of original and modified three lobe bearings at 1480 rpm



ASIA TURBOMACHINERY & PUMP SYMPOSIUM
12 - 15 MARCH 2018
SUNTEC SINGAPORE

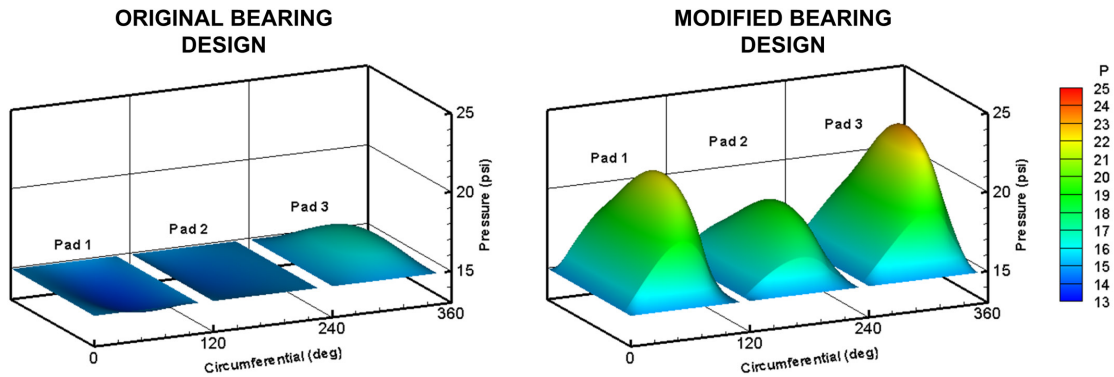


Figure 17: Film pressures within original and modified bearings at 1480 rpm

No significant change in principle damping levels occur going to the modified design. This is due to the fact that the *average* film thickness around the modified bearing's clearance profile is almost identical to the original bearing.

The stability spectrum in Figure 18 illustrates the expected rotordynamic improvements with the modified bearing design. Both forward rotor modes shift from being unstable with negative log decrements using the original bearings to highly stable with log decrements over two. Therefore, the oil whirl instability should be totally eliminated, while the bearing modification should have little impact on the lightly damped casing reed modes.

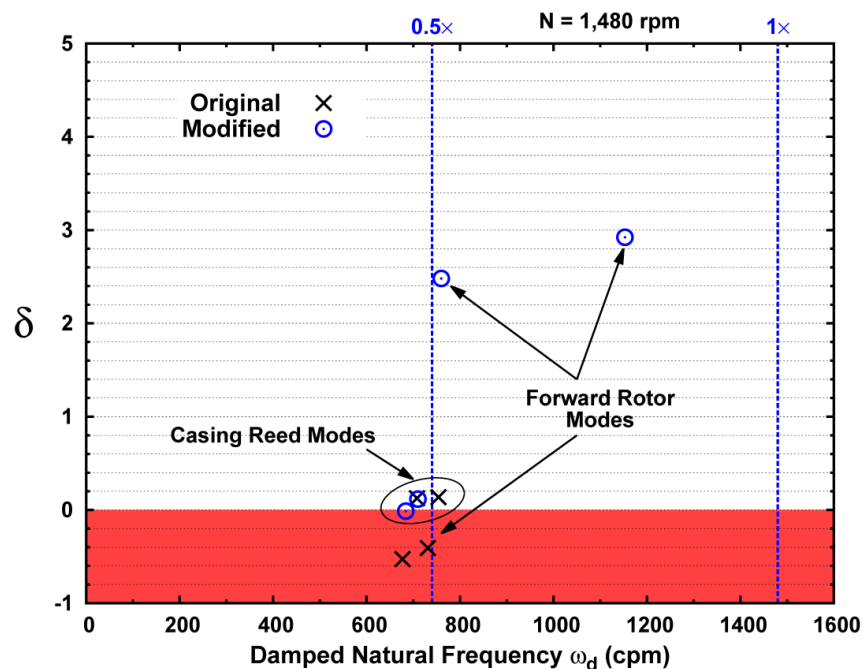


Figure 18: Stability spectrum comparing modes of concern with original and modified bearings



ASIA **TURBOMACHINERY** & **PUMP** SYMPOSIUM
12 - 15 MARCH 2018
SUNTEC SINGAPORE

FINAL TESTING

Due to the geometrical complexity with associated tight tolerances, some manufacturing adjustments were required to obtain the proper geometry. Before their installation inside the bearing housings, all the new sleeves were checked from a dimensional standpoint using a dedicated 3 axis measurement machine. The main geometrical parameters were the clearances (side rails and trailing edges), the lobe radii and centered locations. A total of 48 identical sleeves were required to equip all 12 pumps, but to cope with manufacturing uncertainties, some spare sleeves were ordered, and only the best geometries were selected and installed.

The first validation was conducted on the motor Unit 11 without the pump assembly. This motor was selected because it was the worse in class, referring to Table 1 and Figure 5. The motor by itself was suspended in the vertical direction to be tested in no load conditions and was equipped with Bently Nevada proximity probes, as well as accelerometers on DE and NDE sides. The test setup is shown in Figure 19.



Figure 19: Motor Unit 11 in no load condition with offset sleeve bearings

The measurements were conducted up to 1800 rpm. Only the one per rev component ($1\times$) linked to the residual unbalance was identified from BN probes and accelerometers. The vibration levels were very small, lower than $10\text{ }\mu\text{m p-p}$ and 1 mm/s rms , and no indication of any subsynchronous instability was detected.

The first complete unit was extensively tested (more than 50 running hours, extreme temperature, more than 20 starts & stops, with and without upper bracing, under tilting condition up 17° from the vertical as shown in Figure 20). During all the testing sequence, the vibrations were recorded from accelerometers and BN probes, and absolutely no subsynchronous vibration was identified. Then the pump was disassembled for bearing inspection and, as expected, no damage was observed. The proximity probes used for this validation program were also removed as not part of the standard package prior re-assembly of the complete unit.



ASIA **TURBOMACHINERY** & **PUMP** SYMPOSIUM
12 - 15 MARCH 2018
SUNTEC SINGAPORE



Figure 20: Complete assembly with new bearing, tilted by 17° , in load condition during final Factory Acceptance Test

Thanks to this extended validation program, the new bearing design was considered fully validated and it was decided to definitively equip all 12 motor-pump assemblies with the three lobe offset sleeve bearing design. Thus the 12 motor-pumps were upgraded, and all units were re-tested in load condition without upper bracing at supplier factory during second quarter 2016. As anticipated, the vibratory behavior was free of any whirling or subsynchronous vibration on all of them.

Finally, the pumps were shipped back to Korea to be re-installed inside the four piles of the semi sub platform. Figure 21 shows the arrangement inside one of the machinery room with three pumps in parallel. Among the commissioning and startup activities, a bump test without upper bracing was conducted for all 12 assemblies considering both transversal directions. The first bending mode was measured from 13.5 to 15.9 Hz, which is higher than half rotating frequency.



ASIA **TURBOMACHINERY** & **PUMP** SYMPOSIUM
12 - 15 MARCH 2018
SUNTEC SINGAPORE



Figure 21: Three pumps finally installed in the machinery room of the semi sub platform

The hydraulic performances of the pumps were measured over the entire operating range from minimum (300 m³/h) flow to rated (750 m³/h) flow and the vibratory behavior was recorded as well. All 12 pumps exhibited very low level of vibrations in the range of 1 mm/s rms only on top casing (NDE X and Y directions) and without any subsynchronous indications.

The rotor whirling and the subsynchronous instability were completely cured thanks to the new bearing design and the pumps became fit for purpose to ensure the stability of the offshore semi sub platform.

CONCLUSION

This paper is undoubtedly a success story describing the resolution of a vibration behavior on very critical pumps whose role is to ensure the stability of a semi submersible platform, and thus the safety of a multi billion asset. Despite the apparent design standard of this vertical electrical motor driven pump or claimed to be, this case clearly shows that you cannot make any impasse on the absolute requirement to test at the factory critical equipment in conditions as close as possible to the reality, to verify not only the overall performance but also the mechanical behavior over the entire operating speed range. This case was particularly complex to resolve for many reasons, not only technical with the lack of proper proximity probes on both ends of the electric motor from the beginning of the design, but also contractual considering the number of intermediates between the end user (the O&G Operator) and the electric motor supplier, being a sub-supplier to the pump supplier, itself being a supplier to the EPC contractor working for the end user, all this chain did not help in a swift resolution of the issue. The detection of this critical issue would not have been possible without performing the above described factory tests, without the perseverance of the rotating equipment engineers who did not rely on the simplistic solution that consisted in installing upper bracing to hold the NDE side, which indeed reduced the casing vibrations by moving away the natural frequency from 12.5 Hz up to roughly 20 Hz. “Fortunately”, despite the additional stiffness brought by the presence of the bracings, the subsynchronous vibrations were still visible from the accelerometer probes, which then fully open the investigation further as described in the paper, and well supported by the rotordynamics analysis studies.

Also, as a lesson learnt from this full investigation and subsequent successful resolution, and in addition to the requirement of full factory tests of critical equipment and appropriate instrumentation such as proximity probes, it has to be reminded the basic negative consequences related to the choice of plain sleeve bearings technology for vertical shafts which are prone to instability, particularly related to oil whirl mechanism at about $0.5\times$, which was precisely the case here. This phenomenon is well described in the literature, and should be taken into consideration when selecting the bearings technology. Here, the new bearing design consisting of a three lobes offset with geometrical preload, was successfully implemented and fully tested on all twelve pumps. It must also be outlined that the electric motor supplier was of course fully involved and contributed decisively to the resolution.

REFERENCES

1. Gunter, Edgar J., Jr (1972) “Rotor-bearing Stability”, Department of Mechanical Engineering, University of Virginia.
2. He, M. (2003) *Thermoelastohydrodynamic Analysis of Fluid Film Journal Bearings*, Ph.D. Dissertation, School of Engineering & Applied Science, University of Virginia.
3. Reinhardt, E., and Lund, J.W. (1975) “The Influence of Fluid Inertia on the Dynamic Properties of Journal Bearings” *Journal of Lubrication Technology*, Vol. 97, pp. 159—167.
4. Fritz, R. J. (1970) “The Effects of an Annular Fluid on the Vibrations of a Long Rotor, Part 1 — Theory,” *ASME Journal of Basic Engineering*, Vol. 92, No. 4, pp. 923—929.
5. Black, H. F. (1979) “Effects of Fluid-Filled Clearance Spaces on Centrifugal Pump and Submerged Motor Vibrations,” *Proceedings of the Eighth Turbomachinery Symposium*, Texas A&M University, pp. 29—34.
6. Lund, J. W. (1974) “Stability and Damped Critical Speeds of a Flexible Rotor in Fluid-Film Bearings,” *ASME Journal of Engineering for Industry*, Vol. 96, No. 2, pp. 509—517.
7. Newkirk, B. L., and Taylor, H. D. (1925) “Shaft Whipping due to Oil Action in Journal Bearings,” *General Electric Review*, Vol. 28, pp. 559—568.
8. Singhal, S. and Mistry, R., (2009) “Oil whirl rotordynamic instability phenomenon— diagnosis and cure in large induction motor,” *Proceedings of the Petroleum and Chemical Industry Technical Conference*, IEEE, Anaheim, CA.
9. “#79 Unstable Vibration of Vertical Pump”, Vibration Database (v_BASE) Committee, The Japan Society of Mechanical Engineers, http://www.jsme.or.jp/dmc/Links/vbase/data_english.html (2016 December).
10. He, M., Cloud, C. H., Byrne, J. M., and Vázquez, J. A. (2015) “Fundamentals of Fluid Film Journal Bearing Operation and Modeling”, *Proceedings of the 44th Turbomachinery Symposium*, Texas A&M University.
11. API Standard 610: Centrifugal Pumps for Petroleum, Petrochemical and Natural Gas Industries
12. ISO 10816-Part 7: Mechanical vibration – Evaluation of machine vibration by measurements on non-rotating parts. Part 7 Rotordynamic pumps for industrial applications, including measurements on rotating shaft
13. API Recommended Practices 684: Rotordynamics Tutorial: Lateral, Critical Speeds, Unbalance Response, Stability, Train Torsionals, and Rotor Balancing.